

Thermal stresses in a non-homogeneous orthotropic infinite cylinder

E. Edfawy^{*1,2}

¹Mathematics Department, Faculty of Science, Taif University, K.S.A

²Mathematics Department, Faculty of Science, Assuit University, Egypt

(Received December 19, 2015, Revised April 11, 2016, Accepted April 15, 2016)

Abstract. The present paper is concerned with the investigation of propagation of thermoelastic media, the finite difference technique is used to obtain the solution for the uncoupled dynamic thermoelastic stress problem in a non-homogeneous orthotropic thick cylindrical shell. In implementing the method, the linear dynamic thermoelasticity equations are used with the appropriate boundary and initial conditions. Thermal shock stress becomes of significant magnitude due to stress wave propagation which is initiated at the boundaries by sudden thermal loading. Numerical results have been given and illustrated graphically in each case considered. The presented results indicate that the effect of inhomogeneity is very pronounced.

Keywords: thermal stress; thermal shock; orthotropic material; thermoelastic medium; wave propagation

1. Introduction

The classical and generalized theories of coupled thermoelasticity are extensively developed due to their many applications in the advanced structural design problems. Therefore, it is crucial to obtain the deformation and temperature distributions in the structures under thermal shock loads. In recent year, the case of suddenly applied thermal loading, thermal deformation and the role of inertia become larger. Since the thermal stress changes very rapidly, the static analysis cannot capture its behaviour. This dynamic thermoplastic stress response is significant and leads to the propagation of elastic stress waves in the solid. Abd-Alla and Mahmoud (2010) discussed the effect of rotation and magnetic field in non-homogeneous orthotropic hollow cylinder under the hyperbolic heat conduction model. Finite difference method used to obtain numerical solutions of magneto-thermoelastic problem in non-homogeneous isotropic cylinder by (Abed-El-Salam *et al.* 2007). Abd-Alla and Abo-Dahab (2009) studied the a generalized magneto-thermo-viscoelastic with and without energy dissipation. The effect of rotation on non-homogeneous thermoplastic hollow cylinder discussed by El-Naggar *et al.* (2003). Abd-Alla *et al.* (2003) studied the thermal stresses in a non-homogeneous thermo- elastic multilayered cylinder. Abd-Alla *et al.* (2003) investigated the effect of rotation on transient thermal stresses of non-homogeneous cylindrical composite tubes. (Abd-Alla *et al.* 1999) discussed the effect of rotation on non-homogeneous cylindrical orthotropic composite thermoplastic tubes. Sadd (2005) used the elasticity: theory,

*Corresponding author, Professor, E-mail: essamedfawy11@yahoo.com

application, and numeric's. (Ding *et al.* 2003) investigated the solutions of a non-homogeneous orthotropic cylindrical shell for axysymmetric plane strain dynamic thermoelastic problems. (Kumar and Mukhopadhyay 2010), studied the effects of thermal relaxation time wave propagation under two-temperature thermoelasticity, A generalized thermoelasticity; solution for cylinders and spheres were investigated by Bagri and Eslami (2007). Propagation of waves studied by Prasad *et al.* (2010). Bagri and Eslami (2008) discussed the generalized coupled thermoelasticity of functionally graded annular disk considered the Lord-Shulman theory. Othman and Singh (2007) studied the effect of rotation on generalized micropolar thermoelasticity for a half-space. Generalized magneto-thermoelasticity in conducting medium investigated by Ezzat and Youssef (2005). Abd-Alla *et al.* (2011) studied the propagation of Rayleigh waves in generalized magneto-thermoelastic orthotropic material subjected to initial stress and gravity. The extensive literature on the topic is now available and we can only mention a few recent interesting investigations in (Abd-Alla *et al.* 2015, Praveen and Amit 2015, Khadidja *et al.* 2015, Ren *et al.* 2014, Ray and Majumdera 2014). The extensive literature on the topic is now available and we can only mention a few recent interesting investigations in (1995-2016). In spite of all these investigations, no attempt has been made yet to study the response of the method to solve the uncoupled dynamic thermo elastic stress problem in a non-homogeneous orthotropic thick cylindrical shell. In implementing the method, the linear dynamic thermo elasticity equations is used with the appropriate boundary and initial conditions, and the elastodynamic problem is solved by using finite difference method. It is shown that a closed-form solution can be obtained for the thermal shock stresses in a non-homogeneous orthotropic thick cylindrical shell. It is noticed that the results, a thermal stress wave occurs due to the thermal shock loading, and this plays an important role on the significant amount of dynamic thermal stresses generated through the wall. Numerical computation is performed by using a numerical inversion technique and the resulting quantities are shown graphically.

2. Formulation of the problem

Let us consider a hollow cylinder subjected to a specific temperature environment with or without external pressure. The inner and outer radius are denoted by a and b , respectively.

The stress-strain-temperature relations are given by

$$\begin{bmatrix} \sigma_{rr} \\ \sigma_{\theta\theta} \\ \sigma_{zz} \\ \sigma_{\theta z} \\ \sigma_{rz} \\ \sigma_{r\theta} \end{bmatrix} = \begin{bmatrix} C_{11} & C_{12} & C_{13} & 0 & 0 & 0 \\ C_{12} & C_{22} & C_{23} & 0 & 0 & 0 \\ C_{13} & C_{23} & C_{33} & 0 & 0 & 0 \\ 0 & 0 & 0 & C_{44} & 0 & 0 \\ 0 & 0 & 0 & 0 & C_{55} & 0 \\ 0 & 0 & 0 & 0 & 0 & C_{66} \end{bmatrix} = \begin{bmatrix} \varepsilon_{rr} - \alpha_r T' \\ \varepsilon_{\theta\theta} - \alpha_\theta T' \\ \varepsilon_{zz} - \alpha_z T' \\ \gamma_{\theta z} \\ \gamma_{rz} \\ \gamma_{r\theta} \end{bmatrix} \quad (1)$$

where C_{ij} are the elastic constants and α_{ij} are the thermal expansion coefficients.

The constitutive Eq. (1), the elastic response of the cylinder must satisfy the dynamic equilibrium equations. The equilibrium equation takes the form

$$\frac{\partial \sigma_{rr}}{\partial r} + \frac{\sigma_{rr} - \sigma_{\theta\theta}}{r} = \rho \frac{\partial^2 u_r}{\partial t^2} \quad (2)$$

The strain components in terms of the displacements u_r , u_θ and u_z are

$$\varepsilon_{rr} = \frac{\partial u_r}{\partial r}, \varepsilon_{\theta\theta} = \frac{1}{r} \left(\frac{\partial u_\theta}{\partial \theta} + u_r \right), \varepsilon_{zz} = \frac{\partial u_z}{\partial z}, \varepsilon_{rz} = \frac{1}{2} \left(\frac{\partial u_r}{\partial z} + \frac{\partial u_z}{\partial r} \right) \quad (3a)$$

$$\varepsilon_{\alpha\alpha} = \frac{1}{2} \left(\frac{\partial u_\theta}{\partial z} + \frac{1}{r} \frac{\partial u_z}{\partial \theta} \right), \varepsilon_{r\theta} = \frac{1}{2} \left(\frac{1}{r} \frac{\partial u_r}{\partial \theta} - \frac{u_\theta}{r} + \frac{\partial u_\theta}{\partial r} \right) \quad (3b)$$

where ρ denoted the density of the material.

The Eq. (3) become

$$\varepsilon_{rr} = \frac{\partial u_r}{\partial r}, \varepsilon_{\theta\theta} = \frac{u_r}{r}, \varepsilon_{zz} = \gamma_{\alpha\alpha} = \gamma_{rz} = \gamma_{r\theta} = 0 \quad (4)$$

Substituting from (4) in (1), we get

$$\sigma_{rr} = C_{11} \frac{\partial u_r}{\partial r} + C_{12} \frac{u_r}{r} - \beta_1 T' \quad (5a)$$

$$\sigma_{\theta\theta} = C_{12} \frac{\partial u_r}{\partial r} + C_{22} \frac{u_r}{r} - \beta_2 T' \quad (5b)$$

$$\sigma_{zz} = C_{13} \frac{\partial u_r}{\partial r} + C_{23} \frac{u_r}{r} - \beta_3 T' \quad (5c)$$

where

$$\beta_1 = C_{11}\alpha_r + C_{12}\alpha_\theta + C_{13}\alpha_z$$

$$\beta_2 = C_{12}\alpha_r + C_{22}\alpha_\theta + C_{23}\alpha_z$$

$$\beta_3 = C_{13}\alpha_r + C_{23}\alpha_\theta$$

We characterized the elastic constants C_{ij} and ρ density of non-homogeneous material by

$$C_{ij} = \beta_{ij} r^{2m} \quad \text{and} \quad \rho = \rho_0 r^{2m} \quad (6)$$

where β_{ij} and ρ_0 are constants and m is a rational number .

Substituting from Eqs. (1), (4) and (5) into Eq. (2), we obtain

$$\frac{\partial^2 u_r}{\partial r^2} + \frac{2m+1}{r} \frac{\partial u_r}{\partial r} - \frac{(\beta_{22} - 2m\beta_{12})}{\beta_{11}} \frac{u_r}{r^2} - \frac{\beta_1}{\beta_{11}} \frac{\partial T'}{\partial r} - \frac{((2m+1)\beta_1 - \beta_2)}{\beta_{11}} \frac{T'}{r} = \frac{\rho_0}{\beta_{11}} \frac{\partial^2 u_r}{\partial t^2} \quad (7)$$

The temperature distribution as

$$T(r,t) = T_0 H(t) = \begin{cases} 0, & t < 0 \\ T_0, & t \geq 0 \end{cases} \quad (8)$$

where $H(t)$ is the Heaviside step function.

3. Initial and boundary conditions

The initial condition, as well as the boundary condition due to the absence of external tractions is

$$u(r,0) = 0, \frac{\partial u(r,0)}{\partial t} = 0 \quad (9)$$

$$\beta_{11} \frac{\partial u(a,t)}{\partial r} + \beta_{12} \frac{u(a,t)}{r} - \beta_1 T'(a,t) = 0 \quad (10)$$

$$\beta_{11} \frac{\partial u(b,t)}{\partial r} + \beta_{12} \frac{u(b,t)}{r} - \beta_1 T'(b,t) = 0 \quad (11)$$

It is convenient to have the above Eq. (7) written in non-dimensional form. To this end, we consider the following transformations

$$\bar{r} = \frac{r-a}{b-a}, U = \frac{u}{b-a}, \bar{t} = \frac{ct}{b-a}, T = \frac{T'}{T_0}. \quad (12)$$

In terms of these non dimensional variables, Eq. (7) can be rewritten into a more convenient form as

$$\frac{\partial^2 U}{\partial \bar{r}^2} + \frac{a}{(b-a)\bar{r}+a} \frac{\partial U}{\partial \bar{r}} - \alpha_1 \frac{U}{((b-a)\bar{r}+a)^2} - \alpha_2 \frac{\partial T}{\partial \bar{r}} - \alpha_3 \frac{T}{(b-a)\bar{r}+a} = \alpha_4 \frac{\partial^2 U}{\partial \bar{t}^2} \quad (13)$$

where

$$\alpha = (2m+1)(b-a), \alpha_1 = \frac{(\beta_{22} - 2m\beta_{12})(b-a)^2}{\beta_{11}}, \alpha_2 = \frac{\beta_1 T_0}{\beta_{11}}, \alpha_3 = \frac{((2m+1)\beta_1 - \beta_2)T_0(b-a)}{\beta_{11}},$$

$$\alpha_4 = \frac{\rho_0 c^2}{\beta_{11}}$$

Also, the initial conditions as well as the boundary conditions due to the absence of external tractions, are non-dimensional form can be rewritten as

$$U(\bar{r},0) = 0, \frac{\partial U(\bar{r},0)}{\partial \bar{t}} = 0 \quad (14)$$

$$\beta_{11} \frac{\partial U(a,\bar{t})}{\partial \bar{r}} + \beta_{12} \frac{(b-a)U(a,\bar{t})}{(b-a)\bar{r}+a} - \beta_1 T_0 T(a,\bar{t}) = 0 \quad (15)$$

$$\beta_{11} \frac{\partial U(b,\bar{t})}{\partial \bar{r}} + \beta_{12} \frac{(b-a)U(b,\bar{t})}{(b-a)\bar{r}+a} - \beta_1 T_0 T(b,\bar{t}) = 0 \quad (16)$$

4. Numerical scheme

A finite difference scheme which is a modification of MacCormack’s scheme is described by Haddow *et al.* (1987). This scheme is a leapfrog scheme. We take the finite difference grids with a spatial interval in the direction and k as the time step, and use the subscript and superscript to denote the discrete points in the direction and the n th discrete time ,respectively. Then the equation of motion (12) expressed in the finite difference as follows

$$U_i^{n+1} = 2U_i^n - U_i^{n-1} + \frac{\rho_1}{\alpha_4} \left[U_{i+1}^n - 2U_i^n + U_{i-1}^n + \frac{\alpha h}{2((b-a)(ih)+a)} (U_{i+1}^n - U_{i-1}^n) - \frac{\alpha_1 h^2 U_i^n}{((b-a)(ih)+a)^2} - \frac{\alpha_2 h}{2} (T_{i+1}^n - T_{i-1}^n) - \frac{\alpha_3 h^2 T_i^n}{(b-a)(ih)+a} \right] \tag{17}$$

where $\rho_1 = \left(\frac{k}{h}\right)^2$.

Now we use (17) with $n=0$ as follows

$$U_i^1 = 2U_i^0 - U_i^{-1} + \frac{\rho_1}{\alpha_4} \left[U_{i+1}^0 - 2U_i^0 + U_{i-1}^0 + \frac{\alpha h}{2((b-a)(ih)+a)} (U_{i+1}^0 - U_{i-1}^0) - \frac{\alpha_1 h^2 U_i^0}{((b-a)(ih)+a)^2} - \frac{\alpha_2 h}{2} (T_{i+1}^0 - T_{i-1}^0) - \frac{\alpha_3 h^2 T_i^0}{(b-a)(ih)+a} \right] \tag{18}$$

Using the same technique as thus by using initial condition, Eq. (18) for any \bar{r} except at the boundary conditions (i.e., $\bar{r}=0$ and $\bar{r}=1$) may expressed as

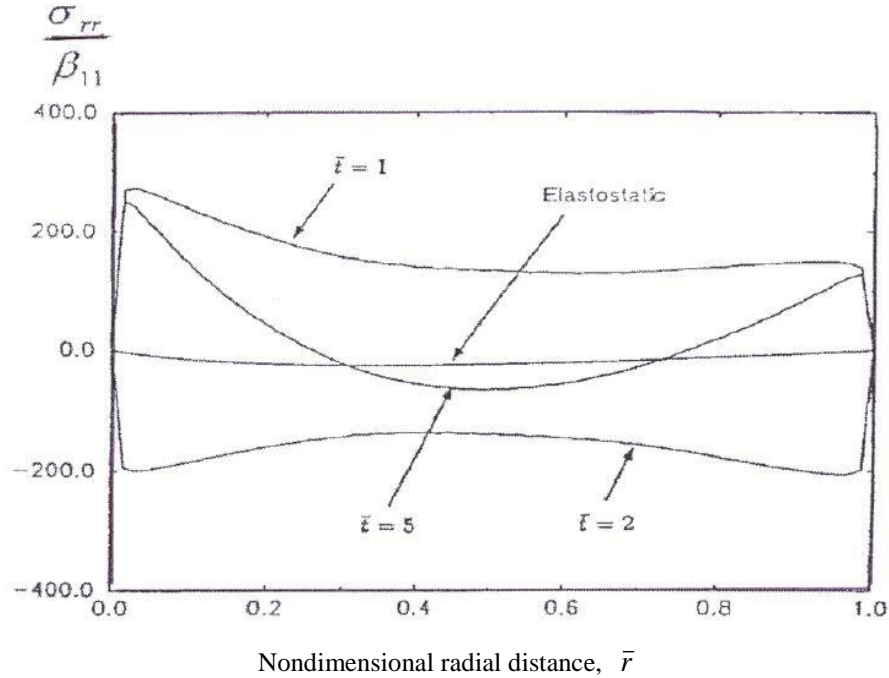
$$U_i^1 = U_i^0 + \frac{\rho_1}{2\alpha_4} \left[U_{i+1}^0 - 2U_i^0 + U_{i-1}^0 + \frac{\alpha h}{2((b-a)(ih)+a)} (U_{i+1}^0 - U_{i-1}^0) - \frac{\alpha_1 h^2 U_i^0}{((b-a)(ih)+a)^2} - \frac{\alpha_2 h}{2} (T_{i+1}^0 - T_{i-1}^0) - \frac{\alpha_3 h^2 T_i^0}{(b-a)(ih)+a} \right] \tag{19}$$

In this case, the second line of values U_i^1 can now be calculated to $O(h^2)$ from the exact values U_i^0 .

Now we are in a position to outline the algorithm for (17) if we now specify the, calculated U_i^1 using (19), the all U are known on the first two lines. When we add the boundary condition at $\bar{r}=0$ and $\bar{r}=1, t>0$, (17) can be calculated point by point, along the third line ($n=2$), then the fourth line ($n=3$), and so on.

5. Numerical results and discussion

As an illustrative example, the disruptions and histories of thermal shock stresses in the wall

Fig. 1 Radial stress distribution ($m=0.5$)

are determined for a glass/epoxy circular cylinder of inner radius $a=50$ mm and outer radius line $b=100$ mm. For the purpose of numerical computation, we take the following values of the constants that are involved in the analysis.

$$\alpha_r = 40 \times 10^{-6} / ^\circ C, \alpha_\theta = 10 \times 10^{-6} / ^\circ C, / ^\circ C, \quad (20a)$$

$$\frac{\beta_{11}}{\beta_{13}} = 1.3535354, \frac{\beta_{12}}{\beta_{13}} = 1.020202, \frac{\beta_{22}}{\beta_{13}} = 6.8080808, \quad (20b)$$

$$\frac{\beta_{23}}{\beta_{13}} = 1.5252525, \frac{\beta_{33}}{\beta_{13}} = 3 \quad \text{and} \quad \beta_{13} = 9.9 \times 10^9 \text{ dynes/cm}^2, \quad (20c)$$

$$\rho_0 = 8954 \text{ g/m}^3$$

To compare the results of this chapter for an isotropic thick cylindrical shell to that of (Kardomateas *et al.* 1998), the material constants are

$$E = E_i = 55.9, \nu = \nu_{ij} = 0.277, \alpha = \alpha_i = 10 \times 10^{-6} / ^\circ C, i = 1, 2, 3 \quad (21)$$

i.e., the constants of the orthotropic shell in the circumferential direction.

The loading temperature of $T(\bar{r}, t)$, causing thermal shock at the surface, is applied at $t=0^+$ over the entire thickness of the hollow cylinder, and it is assumed that the applied temperature is kept constant thereafter. This type of thermal loading, causing the response of strong, dynamic thermal stresses on the cylinder, can be developed by a strong chemical reaction, an absorption of

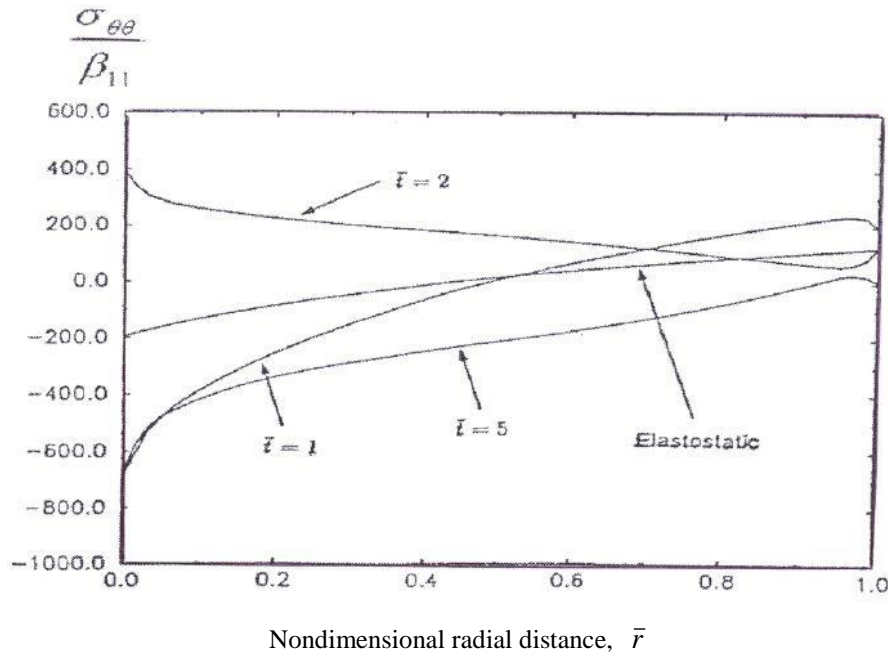


Fig. 2 Hoop stress distribution ($m=0.5$)

infrared radiation, or an electromagnetic radiant energy from pulses.

Fig. 1 shows the variation of normal stress with distance r . Impact of thermal stresses is quite evident on normal stress in both the cases (orthotropic material or isotropic). It is noticed that the pair of curves with rotation (and the pair without thermal stresses) follow opposite oscillatory behaviour. Without rotation, amplitudes of oscillations are higher and increase monotonically. Temperature keeps the trends similar but a significant difference in their magnitudes is noticed. Anisotropy tends the variations to move in opposite oscillatory manner. The distribution of radiant dynamic thermal stress is presented at each non dimension time $\bar{t}=1,2$ and 5 in Fig. 1 Since the speed of the wave c is calculated as 3.169 m/Sec. The non dimensional time $\bar{t}=1$ indicates 1.577×10^{-5} Sec. The radial stress wave is initiated at the inside and outside boundaries simultaneously, propagates outward from the inside boundary and inward from the external boundary through the wall and is reflected in the opposite direction towards the boundary. Subsequently, this reflected wave is also reversed again at the boundaries. It is seen that a large amount of stress variation through the wall exists in an orthotropic cylindrical shell (Fig. 1).

Fig. 2 exhibits the induced thermal stress effect with distance r . Here in all the cases, trend is similar. There is a sharp decrease for the range and then a smooth increase is noticed i.e., behaviour is oscillatory in the rest. Temperature effect causes a change in magnitude of amplitudes. Thermal stress also alters the magnitude of thermal stress effect in descending trends as r increases. Thus, the peaks near the boundaries are much higher than those in other locations. The magnitude of radial stress in an orthotropic cylindrical shell drops near the centre and has an oscillatory behaviour attributed to the direct contribution of static stress and the orthotropic characteristics of elastic constants and thermal expansion coefficients. The largest change of stresses through the shell thickness is observed in the circumferential direction during the first

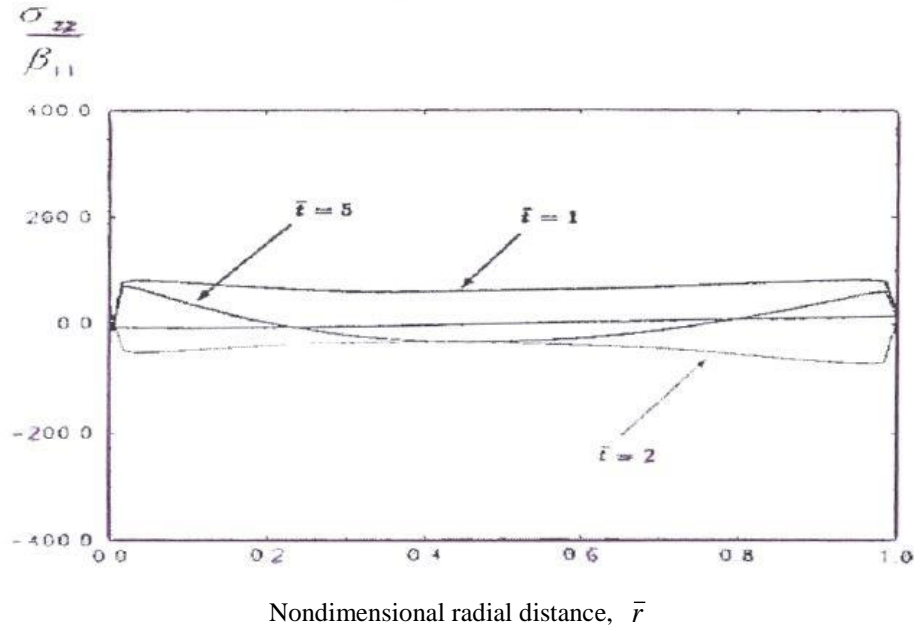


Fig. 3 Axial stress distribution ($m=0.5$)

travel of the wave, as shown in Fig. 2. The magnitude of the hoop stresses near the boundaries increases with continuing wave propagation. The hoop stress near the midpoint in the wall is lower than that near the boundaries. The maximum dynamic thermal stress on a circumferential wound orthotropic cylindrical shell occurs in the first travel in the circumferential direction at the inner boundary. This observation for an orthotropic cylindrical shell is still true as in the isotropic case which was observed in (Wang 1995). It should be noted that the cylinder is most resistant in this direction, since it is circumferentially filament wound and the material strength in the fiber direction is usually the largest. Therefore, this dominant material characteristic affects to a large extent the elastodynamic response of the cylindrical shell structure. Of course, in addition to the stiffness and strength in the fiber direction, the thermal expansion coefficients are also important factors in determining the thermoelastic behaviour of an orthotropic thick cylindrical shell.

Fig. 3 exhibits the variations of axial stress with distance r . Temperature effect alters the magnitude of axial stress without changing the trends. Also a significant difference in the axial stress is noticed for different values of thermal stress. Orthotropic and isotropic variations move in opposite oscillatory pattern. Conductive temperature with radial r is examined in the Fig. 4. The axial stress in Fig. 3 is not significant in comparison with the radial and hoop stresses. Actually, the behaviour of axial stress is similar to that of the radial stress. The tension in the first phase of travel is reversed into compression by the reflection of waves, as shown in Fig. 4, and a dramatic change of radial stress through the thickness is observed. This effect is reduced with time. The first maximum peak radial stress is obtained at $\bar{r}=0.5$ when $\bar{t}=5.5$. As expected, the magnitude of dynamic radial stress is much higher than that in the static case. The time history of the radial stress is shown at $\bar{r}=0.5$ in Fig. 4 (notice the high frequency oscillations). The peaks of radial stress appear whenever the stress wave reaches the corresponding locations. The steep change of magnitude of radial stress is seen near each observing location. A comparison of σ_r at $\bar{r}=0.5$ for

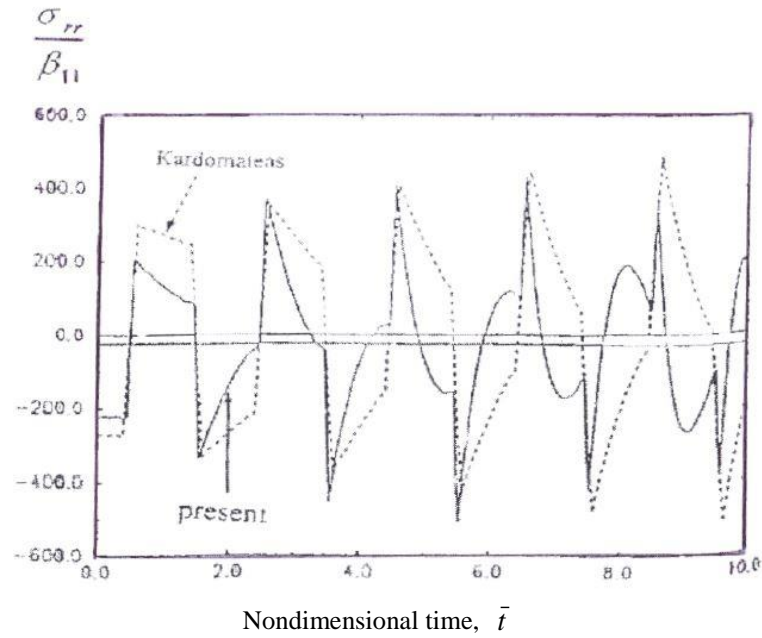


Fig. 4 Comparison of the time history of radial stress ($m=0.0$), with the results of Kardomateas (1998)

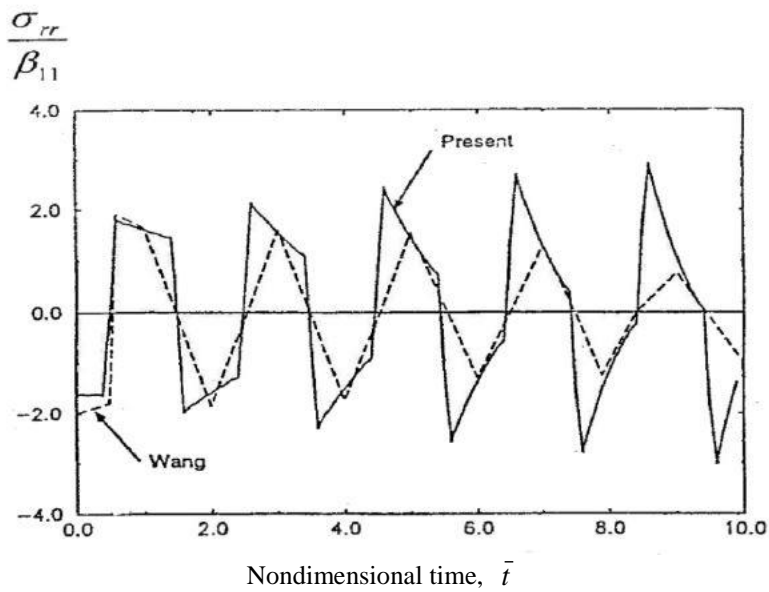


Fig. 5 Comparison of radial stress distribution for the isotropic case ($m=0.0$), with the results of Wang (1995)

the homogeneous orthotropic case, was made with the results of Kardomateas *et al.* (1998), is shown in Fig. 4. One of the differences between the two studies is that a plane-strain condition, was imposed in that study, unlike the present one.

Also, a comparison of σ_{rr} at $\bar{r}=0.5$, for the homogeneous isotropic case, with the results of

Wang (1995) is shown in Fig. 5. The differences between the two results, however, most likely should be due to the differences in the calculation points. The peak values of Wang's (1995) solution are on the present study's curves, but the wave patterns are different after the first trip. This seems to be due to the fact that the plot in Wang (1995) was made from data at time values, not close enough, there for missing the peak values of the stress wave. This comparison also makes an important point: that the time scale of calculations of the data points should be carefully examined to make sure the entire response of the stress wave and especially the peaks are captured.

Fig. 5 exhibits normal normal stress with distance t . Here in all the cases, variations are similar with difference in magnitude. Amplitude of oscillation is maximum in the range and decrease monotonically afterwards

In the study, it should be mentioned that the coupling effects between the thermal and mechanical energy in the system are neglected. This means that the uncoupled linear dynamic thermo elasticity problem was handled. Since the coupling effects always exist in the physical system under thermal environments, the coupled dynamic thermo elasticity is more realistic, but too difficult and complex or some- times impossible to obtain the closed-form solution. The uncoupled dynamic thermo elasticity problem, which was treated here, is, however, still valuable and can provide a large amount of useful information on the thermal shock effects. While studying the rest of the case, we find that all the three follow wave form with difference in magnitudes. These results obey the physical properties of thermoelasticity theory.

6. Conclusions

The analysis of graphs permits us some concluding remarks

1. The medium deforms due to the application of normal/thermal point source or uniformly distributed force/thermal stress effects with vacuum on physical quantities.
2. The thermodynamic temperature and conductive temperature have significant effect on the resulting quantities.
3. The stress decreases when two temperatures coincide. The curves of the stresses is uniform.
4. The normal stresses component show an oscillatory nature with decreasing amplitude with respect to r and due to presence of thermal stress.

References

- Abd-Alla, A.M. and Abo-Dahab, S.M. (2009), "Time-harmonic sources in a generalized magneto-thermo-viscoelastic continuum with and without energy dissipation", *Appl. Math. Model.*, **33**, 2388-2402.
- Abd-Alla, A.M. and Mahmoud S.R. (2010), "Magneto-thermoelastic problem in rotating non-homogeneous orthotropic hollow cylinder under the hyperbolic heat conduction model", *Meccanica*, **45**, 451-461.
- Abd-Alla, A.M., Abd-Alla, A.N. and Zeidan, N.A. (1999), "Transient thermal stresses in a rotating non-homogeneous cylindrically orthotropic composite tubes", *J. Appl. Math. Comput.*, **105**, 253-269.
- Abd-Alla, A.M., Abd-Alla, A.N. and Zeidan, N.A. (2003), "Thermal stresses in a non-homogeneous orthotropic elastic multilayered cylinder", *J. Therm. Stress.*, **23**, 413-428.
- Abd-Alla, A.M., Abo-Dahab, S.M. and Bayones, F.S. (2015), "Wave propagation in fibre-reinforced anisotropic thermoelastic medium subjected to gravity field", *Struct. Eng. Mech.*, **53**, 277-296.
- Abd-Alla, A.M., Abo-Dahab, S.M. and Hammad, H.A.H. (2011), "Propagation of Rayleigh waves in

- generalized magneto-thermoelastic orthotropic material under initial stress and gravity field”, *Appl. Math. Model.*, **35**, 2981-3000 .
- Abd-Alla, A.M., El-Naggar, A.M. and Fahmy, M.A. (2003), “Thermal stresses in a rotating non-homogeneous orthotropic hollow cylinder”, *Heat Mass Transf.*, **39**, 625-629.
- Abd-El-Salam, M.R., Abd-Alla, A.M. and Hosham, H.A. (2007), “Numerical solution of magneto-thermoelastic problem in non-homogeneous isotropic cylinder by the finite-difference method”, *Appl. Math. Model.*, **31**, 1662-1670.
- Ait Yahia, S., Ait Atmane, H., Houari, M.S.A. and Tounsi, A. (2015), “Wave propagation in functionally graded plates with porosities using various higher-order shear deformation plate theories”, *Struct. Eng. Mech.*, **53**(6), 1143-1165.
- Bagri, A. and Eslami, M.R. (2007), “A unified generalized thermoelasticity; solution for cylinders and spheres”, *Int. J. Mech. Sci.*, **49**, 1325-1335.
- Bagri, A. and Eslami, M.R. (2008), “Generalized coupled thermoelasticity of functionally graded annular disk considering the Lord-Shulman theory”, *Compos. Struct.*, **83**, 168-179.
- Belabed, Z., Houari, M.S.A., Tounsi, A., Mahmoud, S.R. and Anwar Bég, O. (2014), “An efficient and simple higher order shear and normal deformation theory for functionally graded material (FGM) plates”, *Compos. Part B*, **60**, 274-283.
- Bennoun, M., Houari, M.S.A. and Tounsi, A. (2016), “A novel five variable refined plate theory for vibration analysis of functionally graded sandwich plates”, *Mech. Adv. Mater. Struct.*, **23**(4), 423-431.
- Benselama, K., El Meiche, N., Bedia, E.A.A. and Tounsi, A. (2015), “Buckling analysis in hybrid cross-ply composite laminates on elastic foundation using the two variable refined plate theory”, *Struct. Eng. Mech.*, **55**, 47-64.
- Bouderba, B., Houari, M.S.A. and Tounsi, A. (2013), “Thermomechanical bending response of FGM thick plates resting on Winkler-Pasternak elastic foundations”, *Steel Compos. Struct.*, **14**(1), 85-104.
- Bourada, M., Kaci, A., Houari, M.S.A. and Tounsi, A. (2015), “A new simple shear and normal deformations theory for functionally graded beams”, *Steel Compos. Struct.*, **18**(2), 409-423.
- Bousahla, A.A., Houari, M.S.A., Tounsi, A. and Adda Bedia, E.A. (2014), “A novel higher order shear and normal deformation theory based on neutral surface position for bending analysis of advanced composite plates”, *Int. J. Comput. Meth.*, **11**(6), 1350082.
- Cho, H., Kardomateas, G.A. and Valle, C.S. (1998), “Elastodynamic solution for the thermal shock stresses in an orthotropic thick cylindrical shell”, *J. Appl. Mech.*, ASME, **65**, 184-193.
- Ding, D.J., Wang, H.M. and Chen, W.O. (2003), “A solutions of a non-homogeneous orthotropic cylindrical shell for axisymmetric plane strain dynamic thermoelastic problems”, *J. Sound Vib.*, **263**, 815-829.
- El-Naggar, A.M., Abd-Alla, A.M., Ahmed, S.M. and Fahmy, M.A. (2003), “Thermal stresses in a rotating non-homogeneous orthotropic hollow cylinder”, *Heat Mass Transf.*, **39**, 41-46.
- Ezzat, M.A. and Youssef, H.M. (2005), “Generalized magneto-thermoelasticity in a perfectly conducting medium”, *Int. J. Solid. Struct.*, **42**, 6319-6333.
- Haddow, J.B. and Mioduchowski, A. (1987), “Dynamic expansion of a compressible hyperelastic spherical shell”, *Acta Mechanica*, **66**, 205-216.
- Hamidi, A., Houari, M.S.A., Mahmoud, S.R. and Tounsi, A. (2015), “A sinusoidal plate theory with 5-unknowns and stretching effect for thermomechanical bending of functionally graded sandwich plates”, *Steel Compos. Struct.*, **18**(1), 235-253.
- Hebali, H., Tounsi, A., Houari, M.S.A., Bessaim, A. and Adda Bedia, E.A. (2014), “A new quasi-3D hyperbolic shear deformation theory for the static and free vibration analysis of functionally graded plates”, *J. Eng. Mech.*, ASCE, **140**, 374-383.
- Kumar, R. and Mukhopadhyay, S. (2010), “Effects of thermal relaxation time on plane wave propagation under two-temperature thermoelasticity”, *Int. J. Eng. Sci.*, **48**, 128-139.
- Mahi, A., Adda Bedia, E.A. and Tounsi, A. (2015), “A new hyperbolic shear deformation theory for bending and free vibration analysis of isotropic, functionally graded, sandwich and laminated composite plates”, *Appl. Math. Model.*, **39**, 2489-2508.
- Marin, M. (1995), “On existence and uniqueness in thermoelasticity of micropolar bodies”, *Comput.*

- Rendus, Acad. Sci. Paris, Serie II*, **321**, 475-480.
- Marin, M. (1999), "An evolutionary equation in thermoelasticity of dipolar bodies", *J. Math. Phys.*, **40**(3), 1391-1399.
- Marin, M. and Marinics, C. (1998), "Thermoelasticity of initially stressed bodies. Asymptotic equipartition of energies", *Int. J. Eng. Sci.*, **36**(1), 73-86.
- Meziane, A.A. (2014), "An efficient and simple refined theory for buckling and free vibration of exponentially graded sandwich plates under various boundary conditions", *J. Sandw. Struct. Mater.*, **16**(3), 293-318.
- Othman, M.I.A. and Singh, B. (2007), "The effect of rotation on generalized micropolar thermoelasticity for a half-space under five theories", *Int. J. Solid. Struct.*, **44**, 2748-2762.
- Prasad R., Kumar, R. and Mukhopadhyay, S. (2010), "Propagation of harmonic plane waves under thermoelasticity with dual-phase-lags", *Int. J. Eng. Sci.*, **48**, 2028-2043.
- Praveen, A. and Amit, S. (2015), "Disturbance due to internal heat source in thermoplastic solid using dual phase lag model", *Struct. Eng. Mech.*, **56**, 341-354.
- Ray, C. and Majumdera, S. (2014), "Failure analysis of composite plates under static and dynamic loading", *Struct. Eng. Mech.*, **52**, 137-147.
- Ren, J.H., Li, Y.S. and Wang, W. (2014), "A penny-shaped interfacial crack between piezoelectric layer and elastic half-space", *Struct. Eng. Mech.*, **52**, 1-17.
- Sadd, M.H. (2005), *Elasticity: theory, application, and numerics*, Elsevier, Amsterdam.
- Tounsi, A., Houari, M.S.A., Benyoucef, S. and Adda Bedia, E.A. (2013), "A refined trigonometric shear deformation theory for thermoelastic bending of functionally graded sandwich plates", *Aerosp. Sci. Tech.*, **24**, 209-220.
- Wang, X. (1995), "Thermal shock in a hollow cylinder caused by rapid arbitrary heating", *J. Sound Vib.*, **183**, 899-906.
- Zidi, M., Tounsi, A., Houari, M.S.A., Adda Bedia, E.A. and Anwar Bég, O. (2014), "Bending analysis of FGM plates under hygro-thermo-mechanical loading using a four variable refined plate theory", *Aerosp. Sci. Tech.*, **34**, 24-34.